Summer 2019 Lab Report

Dalton Glenny, Jingjing Huang, Samantha Livermore
August 20, 2019

Contents

1   Abstract

The purpose of this summer research was to see if we could grow NiO in our lab by evaporating Ni onto different metallic substrates in an O_2 atmosphere, and to measure the resulting change in resistance across the sample on Ni and Cu substrate. We also set out to determine what conditions it would take to grow NiO successfully. The nickel oxide was successfully formed by resistive thermal evaporation in an oxygen atmosphere. The effect of NiO adsorption on surface resistivity of Cu and Ni substrates showed totally opposite trends; however, the experimental results suggest that for both substrates, in the sub-monolayer cover range, it is possible that the surface resistivity change depends on the coverage of NiO adsorbate on the substrate. Likewise, there appears to be a "turning point" in the resistivity change on both substrates that may occur at the point when adatoms start to form a second layer.

2   Experiment procedures and sample preparations

2.1   Sample preparation

The samples we used were cut from silicon wafers with a silicon dioxide surface. The first step in the preparation process is to cut $1cm$ x $3cm$ pieces of the Si wafers with a diamond-tipped scribe. Dimensions slightly smaller than those specified are preferable because samples that are too large will not fit between the two rows of screws on the sample mount, and could potentially stick out from the mount and get caught inside the load lock.

Next, we cleaned our newly cut samples by shaking them in a beaker with $10mL$ of Alconox detergent and $490mL$ of distilled water for fifteen minutes. Typically we would use an ultrasonic cleaner, but due to technical issues, we had to shake the samples in the solution by hand. We then removed the samples from this solution and rinsed them three times with distilled water to remove the detergent, then put them back into beakers with distilled water and shook them for another fifteen minutes [11].

We then placed the samples on an evaporation mount, leaving only the right and left sides of the sample exposed for contact deposition. We then put the samples into a bell jar evaporation chamber so that we can deposit Ag contacts in a clean environment. At this point, we attempted to deposit $100\mathring{A}$ of Cr and $500\mathring{A}$ of Ag, but because our quartz crystal was cracked in the QCM, we got unreliable deposition amounts. Once we removed the samples from the evaporation chamber and the sample mount, we pressed scotch tape against the contacts to see if the Ag layer would come off or not. If they were easily removed from the sample, we would know that the contacts were not sticking sufficiently to the Si/Cr surface. If the contacts stayed in tact, they are ready for our use in experiments in the UHV [11].

2.2   Oxygen exposure procedure

In order to create an O_2 atmosphere, we let in O_2 through a valve connected to the gas manifold rather than sending the O_2 through a doser; using the doser may have helped with reducing contaminant levels on the sample surface. We monitored the pressure of O_2 during our experiment by observing a pressure vs. time RGA reading.

2.3 Nickel and copper deposition procedure

In our experiments, nickel and copper are deposited with a set of pre-outgassed filaments using resistive thermal evaporation. During the deposition, the sample temperature is regulated at $296 \pm 1K$ with liquid nitrogen and a PID controller.

3 Calibration of sample coordinates

3.1 Experiment

We used Auger electron spectroscopy to determine the z-coordinates of the edges of the sample; we hypothesized that when we approached each edge, the Auger scan would get noisier due to the energetic Auger electrons not reflecting back cleanly from the edge. We moved in $\sim 0.050mm$ increments and found that the points with the highest noise to Ni peak ratio were about $\sim 1cm$ apart, which is the known width of the sample.

3.2 Results and analysis

Noise and peak ratios for each position [1] are calculated and plotted in **Fig.1**. The peaks were found at $z = 0.350$ and $z = 0.740$, thus we believe them to be the top and bottom edges of the sample. The z-coordinate of center of the sample can be obtained by:

$$\frac{z_{lower} + z_{upper}}{2} = \frac{0.350 + 0.740}{2.00} = 0.545.$$

According to this coordinate, and the known size of the sample, the lower and upper positions for AES scans are estimated to be at $z = 0.445$ and $z = 0.745$.
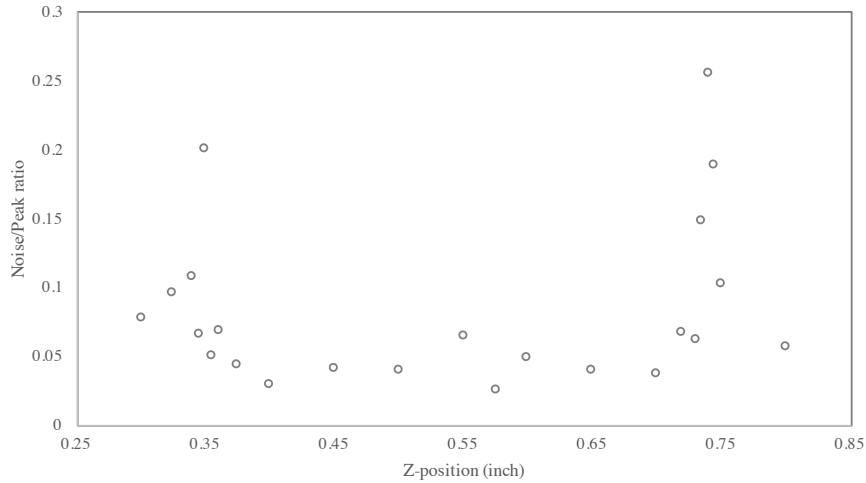

Fig.1: Noise/Peak ratio versus z-axis position
(<u>Note</u>: Auger ratios average of 05JE19_A.aug and 05JE19AL.aug).

4   Oxygen exposure on substrate

In oxygen exposure experiments, we expect to see an increase in the resistance of the sample. Scattering of conduction electrons on the surface by oxygen causes the change in surface resistivity, $\Delta\rho$. For the case of uniform adsorption behavior on metal substrate, $\Delta\rho$ can be expressed by the following equation [2]:

$$\frac{\Delta\rho}{\rho_B} = \frac{3}{16}\frac{l_B}{t}\Sigma n,$$

where ρ_B is bulk resistivity, l_B is the electron mean free path, t is the thickness of the substrate, Σ is the scattering cross section for each adsorbate, and n is the surface density of adsorbate.

Since the scattering cross section is constant for a pure substance adsorbate, $\Delta\rho$ is expected to have a linear dependence on the density of the adsorbate, i.e., the coverage of O on the surface. When O saturates on the surface and starts to grow a second layer, the resistivity should stop increasing since the second layer adsorbate is not able to interact with the conduction electrons of the substrate.

4.1   Experiment: On a complex nickel surface

The sample surface used in this experiment is complicated as it has undergone various metal depositions and has been sputtered many times, and it has been sitting in the chamber for a long time. As such, it is not possible for us to know the exact components and thickness of the substances on the sample, and no serious scientific result will be obtained from experiments on this complex Ni surface. The experiments in Section 4.1 are mainly for our research group to practice and learn experimental procedures.

4.1.1   Results and analysis

We took an AES scan before the experiment to get a baseline of the composition of the surface. The results showed that the surface contains carbon, nitrogen, oxygen, and nickel, and the peak ratios were calculated to find the relative amount of each element (the largest peak for Ni at $848eV$ was used as the denominator in each calculation):

$$\frac{[C]}{[Ni]} \approx 0.30, \quad \frac{[N]}{[Ni]} \approx 0.024, \quad \frac{[O]}{[Ni]} \approx 0.12.$$

(<u>Note</u>: Auger ratios average of 17JE19_G.aug and 17JE19_H.aug)

After getting a baseline of component ratios, the sample is ready to be exposed to O_2. During the exposure we ran an RGA pressure vs. time scan and an LIA scan. We noted a negative linear drift in the LIA signal before beginning the experiment. We let in oxygen at approximately $470s$; this corresponded with the start of the voltage increase visible in the **Fig.2** (plotted from $17JE19\_C.lvm$). We left the leak valve open to keep O_2 at a pressure of $\sim 10^{-6}Torr$ for $200s$. The LIA signal plateau corresponds to the shutting of the leak valve.
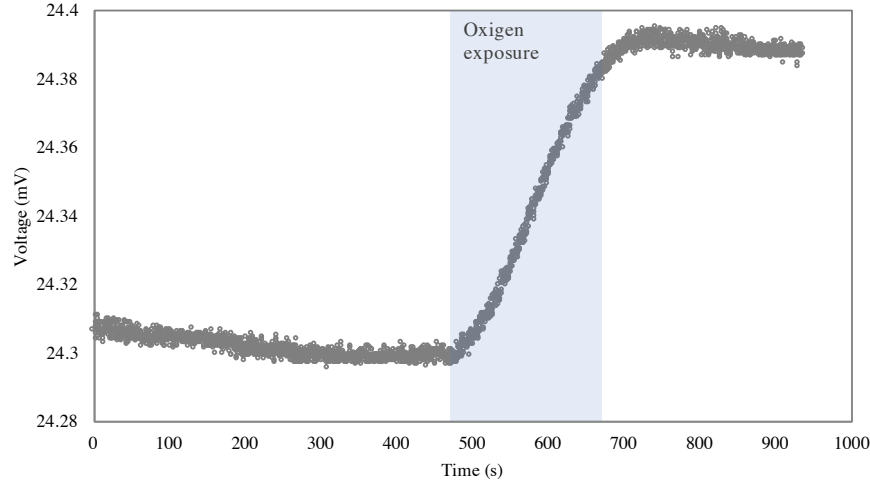
Fig.2: Voltage across sample changing during $200L$ O_2 exposure on 17 June ($P_{O_2} \approx 10^{-6} Torr$, $t = 200s$, data from $17JE19\_C.lvm$)

After the experiment, we took another AES scan to see how much oxygen was adsorbed onto the surface:

$$\frac{[C]}{[Ni]} \approx 0.23, \quad \frac{[N]}{[Ni]} \approx 0.029, \quad \frac{[O]}{[Ni]} \approx 0.49.$$

(<u>Note</u>: Auger ratios average of 17JE19_I.aug through 17JE19_M.aug)

Note that though the $\frac{[C]}{[Ni]}$ and $\frac{[N]}{[Ni]}$ did not change, the $\frac{[O]}{[Ni]}$ ratio increased by a factor of four, which is much to be expected from exposing this surface to an oxygen atmosphere.

4.1.2 Conclusion and questions

The difference in $\frac{[O]}{[Ni]}$ ratio before and after the O_2 exposure supports the conclusion that the oxygen adsorption on the surface was successful. According to the LIA graph, there was an increase of about $0.08mV$ after exposing $200L$ of O_2 to the sample surface. It is known that the current in the four-terminal sensing circuit is $2mA$, and the change in resistance of the sample can be obtained easily using Ohm's Law:

$$\Delta R = \frac{\Delta V}{I} = \frac{0.08 \times 10^{-3} V}{2 \times 10^{-3} A} = 0.04\Omega$$

We expected to see an increase in resistance in response to the oxygen exposure, which was confirmed by the calculation above. We cannot conclude based on the LIA scan that the oxygen formed a saturated monolayer on the surface, as the plateau behavior seen in Fig.2 corresponds to shutting the leak valve rather than O_2 saturation.

We did not see the indicator for oxygen saturation on the surface, namely that the shape of the LIA scan would plateau off as the O_2 monolayer saturates. Since $200L$ is a very large dose for this surface, the oxygen should be fully saturated if we can trust our exposure calculation.

Due to an issue of incorrectly measuring the pressure of oxygen during this experiment, we cannot be sure of our exposure calculation. However, the actual exposure is still in the range of 10^2L. Since there is no plateau on the LIA graph during O_2 dosing, it is possible that although the exposure is large, not enough oxygen

adsorbed onto the surface, i.e., the sticking coefficient of this system is very small. Further evidence of this can be found in the Auger ratio $\frac{[O]}{[Ni]}$. According to Holloway's paper, the oxygen peak increases linearly at temperatures of $302K$ before $80L$ for a clean Ni surface, which means that the coverage of oxygen on the surface increases linearly during the first $80L$ exposure.[4] If the error of oxygen pressure, low sticking coefficient, and complexity of surface in our system are factored in, it is reasonable that the saturation of oxygen on the surface cannot be observed during this experiment.

Time permitting, we had planned to do another oxygen exposure at a different pressure to try to increase the oxygen adsorption rate. We would also have changed the way we measured the oxygen pressure to get a more accurate measurement; however, due to technical difficulties, we were unable to run this experiment.

4.2   Experiment: On clean copper surface

We repeated this experiment four times; however the results have been different each time. This may be due to some variables changing; they will be discussed in section 4.2.2.

The sample surfaces used in this set of experiments are very clean Cu surfaces. The samples are prepared by depositing about $300\mathring{A}$ Cu on a single crystal SiO_2/Si surface, and an AES scan is done before each experiment to make sure the surface is pure Cu.

4.2.1   Results and analysis

The first two experiments were done with bad electrical contacts which resulted in unreliable voltage measurement. Despite this issue, the trends of the LIA graphs for these experiments reasonably matched the shapes of the two later, successful experiments, so we have elected to include them here:
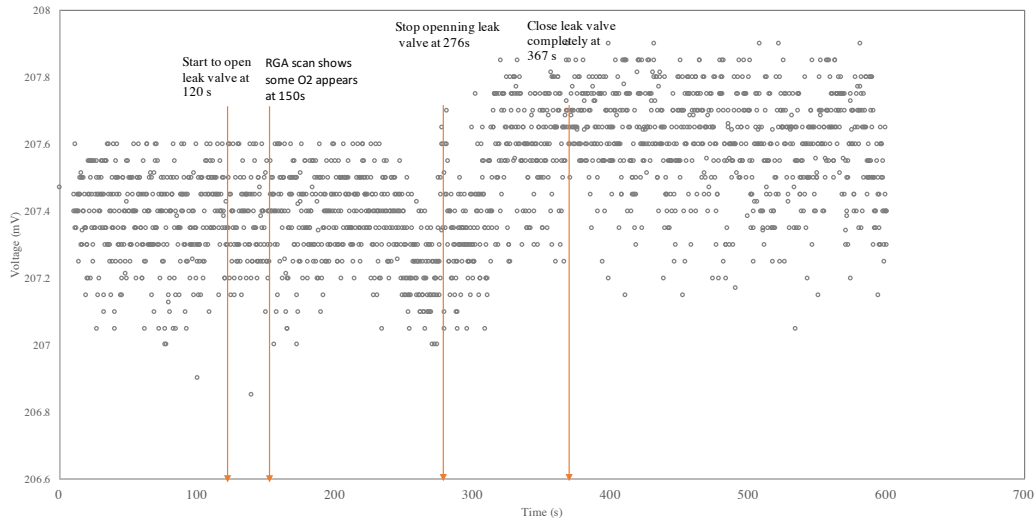

Fig.4(a): Voltage across sample changing during the oxygen exposure on 11 July ($11JL19\_D.lvm$). (and the LIA graph from the experiment on 16 July ($16JL19\_B.lvm$) showed extremely similar pattern like this one.

After the first two experiments, we vented the chamber and removed the sample mount to fix the contact

problem, and then we were able to continue with the third and fourth experiments. For these, the exposures of oxygen were $\sim 100L$ and $10L$ respectively. The voltage changes are shown in **Fig.4(a)** and **Fig.4(b)**:
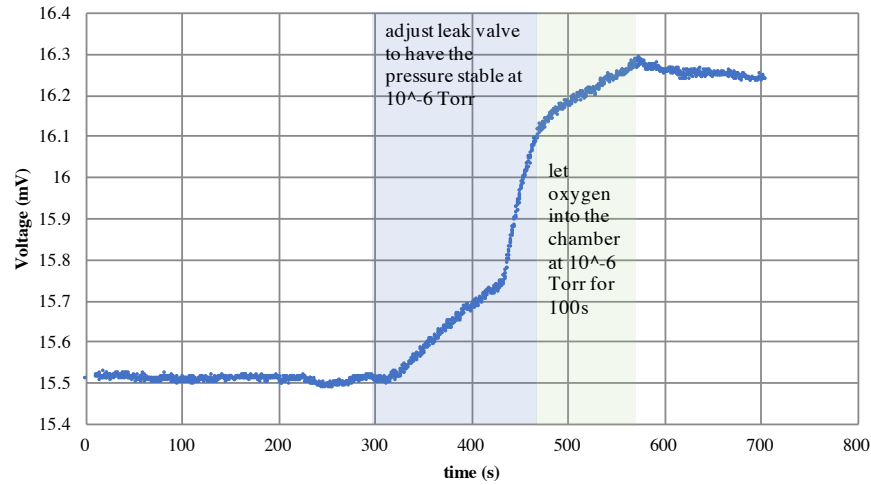

Fig.4(a): Voltage across sample changing after $120L$ O_2 dosing (includes the exposure during adjusting leak valve). This was our third experiment on Cu.
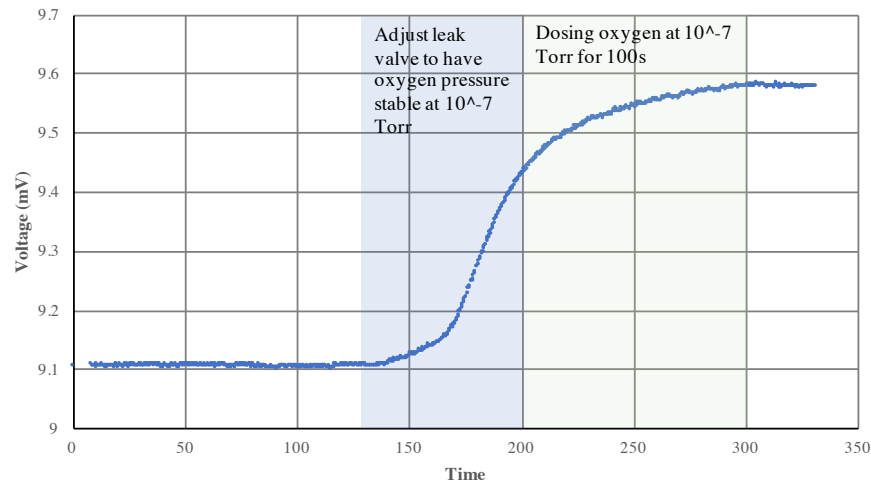

Fig.4(b): Voltage across sample changing after $10L$ O_2 dosing (includes the exposure during adjusting leak valve). This was our fourth experiment on Cu.

In the process of exposing the sample to oxygen, we consistently observed the presence of CO (about $\frac{1}{3}$ of total pressure) in the gas influx; the CO pressure was usually unstable. As a result, it was not easy to adjust the leak valve to stabilize the oxygen pressure, which meant that the actual exposure was always a little larger than planned. However, the result of voltage change is still confusing, even considering these challenges.

The voltage change after dosing $\sim 120L$ O_2 was about 0.75 mV, and the voltage change after dosing $\sim 12L$ O_2 was about $0.47 mV$.

All four experiments are summarized in **Table 1**. Note that despite the poor electrical contacts, the voltage changes across samples 1 and 2 are in the same range and order of magnitude as the following two samples, so they have been kept in the table for posterity. This is also true of their Auger ratios.

Samples	O_2 Pressure (Torr)	Time elapsed (s)	Voltage change (mV)	$\frac{[O]}{[Cu]}$Auger peak ratio	Note
1	7.3×10^{-8}	100	0.45	0.11	Bad contact
2	8×10^{-8}	100	0.4	0.14	Bad contact
3	10^{-6}	100	0.75	<0.23	No AES was done
4	10^{-7}	100	0.47	0.14	

Table 1: Results for four oxygen dosing experiments on four different samples.

<u>Note</u>: Auger ratios average of the following:
sample 1: 11JL19_U.aug through 11JL19_Y.aug
sample 2: 16JL19_E.aug through 16JL19_I.aug
sample 3: 30JL19_G.aug
sample 4: 02AU19_G.aug through 02AU19_K.aug

<u>Note</u>: for sample 3, no Auger scan was done immediately after the first oxygen exposure (this was just human error), though one was done later after a second oxygen exposure, which is the source of the <0.23 threshold.

4.2.2 Conclusion and questions

We expected to expose more oxygen to sample 3 than to previous samples in order to see convincing evidence of saturation so that we could do NiO deposition on that surface; however, after exposing oxygen at about $1.2 \times 10^{-6} Torr$ for $600s$, the voltage still showed no signs of leveling off (**Fig.5**). Note that the leveling off that can be seen in **Fig.4(a)** was due to closing the leak valve, which can be seen in the discontinuity, whereas in **Fig.4(b)** it looks as though the oxygen had saturated before we shut the leak valve.

One possible reason for the failure of the oxygen to saturate on sample 3 is potential contamination during the exposure; pure oxygen should saturate at the given exposure. AES scans showed that there was also some nitrogen on the surface, and the Auger ratios for sample 3 were:

$$\frac{[N]}{[Cu]} \approx 0.28, \quad \frac{[O]}{[Cu]} \approx 0.23.$$

(<u>Note</u>: Auger ratios from 30JL19_G.aug)

The presence of nitrogen in the chamber is not itself remarkable, since it was used immediately before this experiment to vent the chamber; however, under room temperature and the absence of catalysis, nitrogen gas does not react with oxygen, and it is also not adsorbed by copper. Though there is little reason to believe that the nitrogen could have interfered with our oxygen exposure, it was the only appreciable difference in this particular experiment.
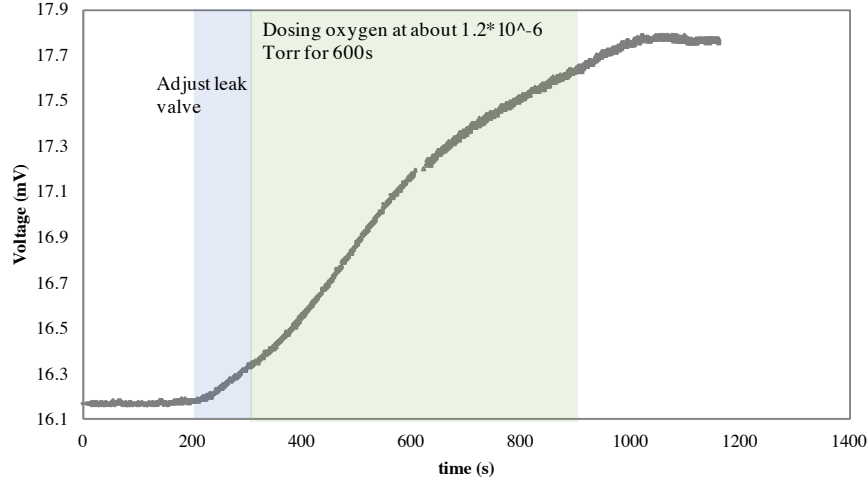
Fig.5: second oxygen exposure on sample 3

4.2.3 Plan for future experiments

To determine clearer dependence between O_2 coverage on a Cu surface and its surface resistivity, further experiments are needed. We planned to expose the sample to O_2 with a doser instead of using leak valve in order to focus the O_2 exposure and reduce contamination, and to use a different exposure to get more effectively O_2 coverage. We would also fully flush all nitrogen from the gas manifold. Due to time constraints and technical issues with our instruments, we were not be able to run this series of experiments during this summer.

5 Temperature dependence of resistance

The temperature of a conductor affects its resistivity. The migration of electrons in a material causes current to flow. The higher the temperature of the conductor, the more violently atoms in the material vibrate, which causes free electrons to collide more with captured electrons. Collisions take some energy and hence reduce the conductivity of the material.

In our experimental setup, the temperature of sample is measured by a thermocouple touching the sample. Some technical constraints of the thermocouple include that there is a time delay in temperature readings (i.e. the reading is not live), and the temperature measurement is only accurate to one decimal place.

Sometimes a fluctuation of voltage across the sample shows up on the LIA graph without making any change to the surface (like deposition or gas exposure), but the temperature monitor shows no change despite the fact that a fluctuation in temperature would be the most likely cause. As such, determining the dependence between the temperature and the resistivity of our sample is particularly important.

5.1 Experiment on Nickel

We cooled the sample using liquid nitrogen, and then heated the sample using the PID controller. Data points were taken every 5^oC, and the resulting voltage vs. temperature relationship is plotted below.

This experiment was done on the complicated Ni surface described in section 4.1.

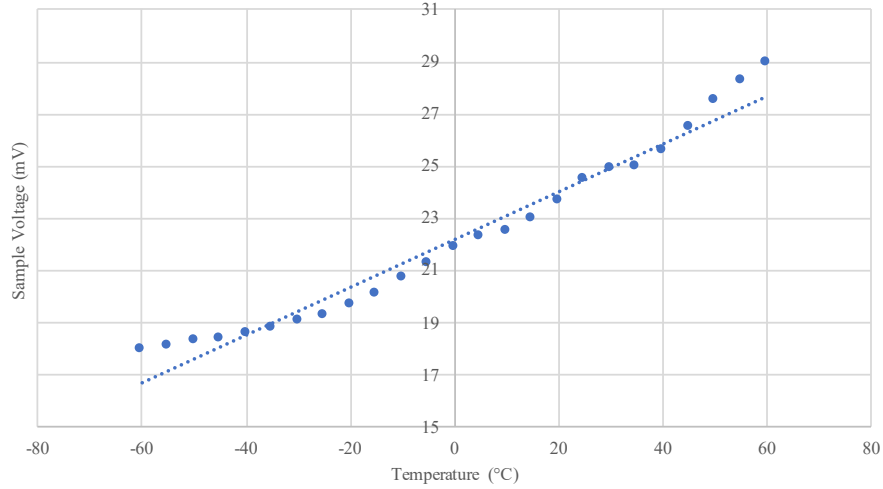## 5.2 Results and analysis

Fig.6: Voltage across nickel sample varying with temperature [5]

It is well known that for a normal conductor, the dependence between temperature and resistance is:

$$R(T) = R(T_0)[1 + \alpha(T - T_0)],$$

where $R(T)$ is the resistance of the conductor at temperature T, $R(T_0)$ the resistance of the conductor at temperature T_0, and α is temperature coefficient of resistance, and the value of α depends on the material of the conductor.

In our experiment, although the material is complex, we can regard it as a normal conductor, so the relation should theoretically be linear. During the experiment, temperature was controlled by varying the current through the sample heater, and the current was adjusted from time to time to keep the temperatures stable. The thermocouple sample temperature measurements were not incredibly precise and needed some time to update with each temperature change. When the current is turned up, the temperature should increase suddenly, but it took some time for the thermocouple to show the change. As such, a nonlinear dependence is suggested in some parts of the graph; however, a linear regression can be done based on the least square method. Choosing $T_0 = 20^oC$, the resistance equation base on temperature is obtained:

$$R(T) = 12.0\Omega[1 + 0.00383^oC^{-1}(T - 20.0^oC^{-1})].$$

The temperature coefficient is 0.00383^oC^{-1}.

Some notes: first, our experimental temperature coefficient is about $.002oC^{-1}$ smaller than the accepted value for bulk film Ni, though we have included it because it is within a reasonable range. Secondly, we intended to repeat this experiment on a Cu surface as well, but we were not able to due to an instrument problem.

6 Nickel Oxide deposition on Nickel surface

6.1 Experiment

We began by sputtering the surface of the sample to clean off existing layers to expose a Ni surface. This method left us with an uneven Ni surface containing other contaminants, as opposed to "cleaning" the surface by covering up the similar complex surface with a thick layer of Cu as described in Section 7.1.

In order to study how NiO changed the resistance of our sample, three experiments were done. All three of them had extremely similar procedures, and most importantly the voltage across the sample was monitored during each experiment. The curves from the LIA graph of each experiment showed similar trends, as portrayed in **Fig.7**. This graph is a good representation of the trends seen across all three experiments.
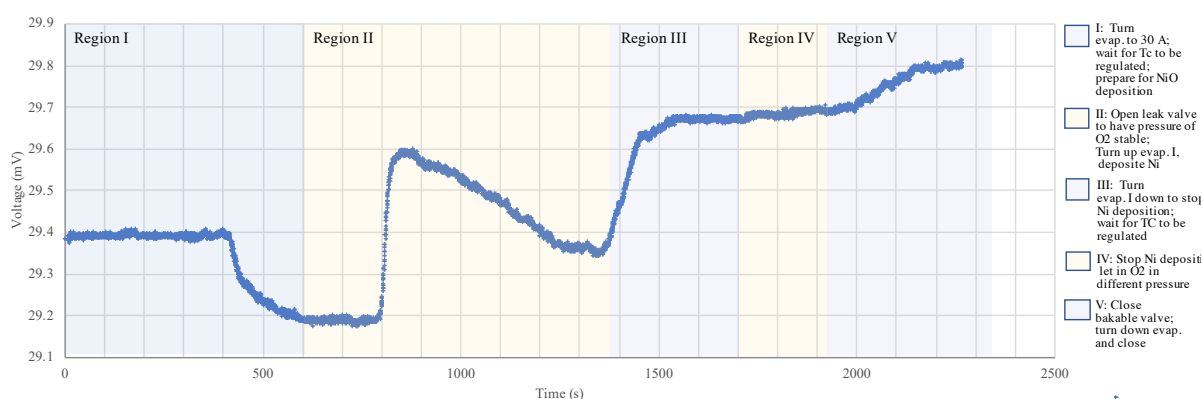

Fig.7: Voltage across sample changing during NiO deposition experiment on the complex Ni surface; filename $03JL19\_C.lvm$

Here are the trends across all three experiments:

In Region I, the current through the filament is turned up to about $30A$ to prepare for Ni deposition. During this procedure, the temperature of substrate tended to fluctuate due to the warming filament. Once the temperature is stably regulated and we observed the beginning of Ni deposition, we created an oxygen atmosphere in the UHV using the leak valve at the start of Region II.

Region II shows how the voltage across the sample changes during NiO deposition. The strong jump in the graph most likely corresponds to the start of NiO deposition. In this time period we raised the evaporation current to the appropriate level for ideal NiO deposition and kept the O_2 pressure as stable as possible. Note: There is one notable disadvantage of using the leak valve to let in O_2: it lets in some amount of unwanted gas (like CO), hence it is hard to control the exact exposure of O_2. However, by observing the RGA pressure vs. time graph, it was observed that the main unwanted gas in the chamber was CO, and that its pressure was about $\frac{1}{2}$ of that of oxygen. Thus, we can roughly estimate the exposure of oxygen from this ratio.

Region III takes place after depositing about $20\mathring{A}$ of NiO. The evaporator current is turned down to a low enough value where the Ni filament can no longer evaporate. The rise in the graph could be from the adsorption of oxygen now that the Ni is no longer evaporating but the oxygen atmosphere still exists.

In Region IV, the pressure of oxygen atmosphere is changed by adjusting leak valve.

Region V includes closing the leak valve and turning off the evaporation filament. Thus, the whole experiment can be split into two parts: the first includes Regions I and II, which shows the effect of NiO deposition on sample resistance. The second part focuses on the oxygen adsorbate effect on the sample resistance of NiO pre-exposed Ni surface.

6.2 Results and analysis

Observing **Fig.7**, the first sudden drop happens while turning the evaporator current up to $30A$; to be more specific, it happens $35s$ to $55s$ after the current is turned up to $20A$. During this period, an obvious increase (about $0.4 \times 10^{-9} Torr$) in total pressure in the chamber is also observed. This evidence shows it is possible that Ni has been deposited much earlier than expected. However, limited literature on the effects of metallic adsorbates on surface resistance suggest that the resistance increases linearly with coverage before the adsorbates start to form a second layer[6][7][8]. If the sudden drop in voltage in Region I is because of adsorption of nickel atoms, the decrease and nonlinearity of the curve of our result conflicts with the two experiments cited[7][8]. However, from the previous experiment of Ni deposition on the complex Ni surface on 7/26, it showed that the resistance of sample decreased during Ni deposition on it.

The second obvious change in resistance is observed in Region II, and it is clearly caused by the exposure to oxygen and nickel evaporation. We assume that evaporating nickel in an oxygen atmosphere causes NiO adsorption on the sample surface at our given pressures based on our Auger scans matching those of NiO in Netzer's paper [9]. During this time, the pressure of oxygen in the chamber is kept in the lower $10^{-6} Torr$ range, and the result shows that there is a strong dependence between surface resistivity and the thickness of adsorbate (**Fig. 7**). It is known that the parameter which primarily affects the surface resistivity is the coverage of the adsorbate, however, monitoring the coverage directly during experiments was not feasible for our lab. Instead, the thickness of adsorbate was monitored by a calibrated quartz-crystal monitor. In our lab, Auger scans were used to determine the coverage of adsorbate on the substrate by looking at the ratios of $\frac{[O]}{[Ni]}$. Due to the complexity of the substrate, it is very hard to evaluate the coverage change of NiO on the substrate quantitatively. As such, only a qualitative result based on thickness of adsorbate is given in this report.

In our experiments, oxygen is let in once $1\mathring{A}$ of Ni is observed by the quartz-crystal monitor, and the resistance then is used as a baseline when we calculate ΔR. And once $18\mathring{A}$ of adsorbate is observed, evaporation current for nickel is turned down until it is off. In the three experiments, the exposure of oxygen was different:

- 06/27: Exposure$\approx 6.2 \times 10^{-7} Torr \times 360s \approx 220L$

- 07/01: Exposure$\approx 1.3 \times 10^{-6} Torr \times 600s \approx 780L$

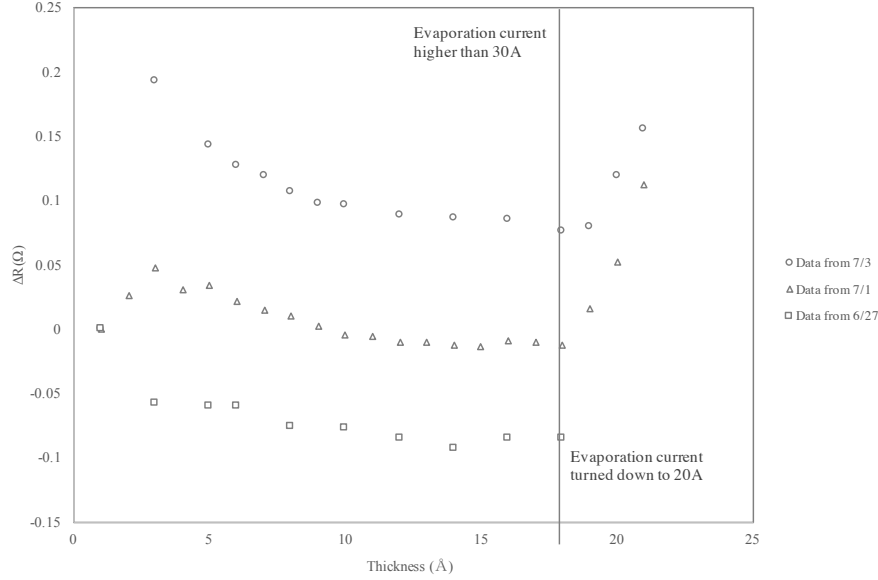- 07/03: Exposure$\approx 1.4 \times 10^{-6} Torr \times 600s \approx 840L$

Fig.8: Resistance change of sample after getting $1\mathring{A}$ of Ni adsorbate in three experiments.

Three experiments showed the same pattern: before $3\mathring{A}$ deposition is seen, the resistance increases quickly; and for data from 7/1, we can see a linear trend. However, data from 6/27 did not show the increase like the other two experiments did, which may be an effect of temperature. During the the time period where $3\mathring{A}$ was observed in that experiment, the temperature monitored by the thermocouple on the sample had risen to $296.75K$, so it is possible that if the temperature had been kept unchanged, a higher resistance may have been measured. At the end of each of the three experiments, when the evaporation current was turned down, the temperature dropped by about $1.5^{o}C$, and the resistances all went up. So combining these two factors, it is possible that the effect of temperature on resistivity change of this sample with NiO adsorbate acts totally different from this sample without NiO adsorbate on it. After $3\mathring{A}$, the resistance starts to decrease and level off at about $13\mathring{A}$ or $14\mathring{A}$. If the assumption about dependence of resistivity and temperature is true, one possibility is that the adsorbate saturated on the substrate when $3\mathring{A}$ is observed by the QCM, and then the adatoms start to grow a second layer.

After every experiment, an Auger scan was done to see the $\frac{[O]}{[Ni]}$ ratio, and compare it to the actual ratio found for NiO surface in Netzer's experiment [9]. It showed that the Auger ratio of $\frac{[O]}{[Ni]}$ for our sample surface is very close to Netzer's ($\sim 2x$ as much O_2 as Ni), therefore, it is a convincing evidence that we have formed NiO on the surface instead of oxygen adsorbed on nickel surface.

6.3   Conclusion and plans

It is difficult to draw any serious conclusions with only three experiments, however, we still can come up with some hypotheses and experiments to verify them:

- Nickel starts to evaporate and be adsorbed onto the substrate when the evaporation current is turned to $20A$. And once the first adatom gets adsorbed on the substrate, there is a sudden drop in resistance, and the dependence of resistance and coverage of Ni substrate is nonlinear. To verify this, some more Ni deposition experiments are needed, as well as a low evaporation current ($\sim 20A$), and a more sensitive QCM setting. It is difficult to determine the coverage of Ni, so we can also do this experiment on a copper surface to see how they differ.

- The resistance of a sample with nickel substrate and NiO adsorbate goes up when the temperature of sample goes down. This can be tested easily with liquid nitrogen and the PID controller.

- The NiO adsorbate forms a monolayer before $3\mathring{A}$ is observed on QCM. In the sub-monolayer range, the sample resistance increases with surface coverage. And after that, the resistance starts to decrease with the thickness of the adsorbate. It would be preferable to have a new, clean nickel surface on which to run this experiment again, with a different oxygen pressure. Also, it would be helpful to use a lower evaporation current to allow us to better monitor the temperature and deposition. We would also stop the deposition before and after seeing $3\mathring{A}$ on QCM, do an Auger scan to see the $\frac{[O]}{[Ni]}$ ratio and narrow down the time range when the adsorbate has saturated for the first monolayer.

7   Nickel oxide deposition on copper surface

7.1   Experiment

To prepare the sample for NiO deposition, we first deposited 300Å of Cu onto the surface to have a simple, clean basis to work off of; we took an Auger scan to confirm the existence of a pure Cu surface. Then we exposed the sample to $\sim 10L$ of oxygen, which was meant to create a saturated monolayer on top of the Cu layer; again, we used Auger to confirm. Only then did we deposit NiO. This was done by evaporating Ni into an oxygen atmosphere. However, we were not able to create a saturated oxygen monolayer on Cu substrate, and never saw voltage across sample level off. We continued and ran the experiment anyway.

This experiment has been run for three times, however, two of them were done with bad electrical contacts which resulted in inaccurate voltage readings. As such, we only used data from the last experiment with good contacts. However in this experiment, there was very little nickel on the evaporation filament, and hence the deposition rate was very low, and at the end, we only got about $10\mathring{A}$ of NiO.
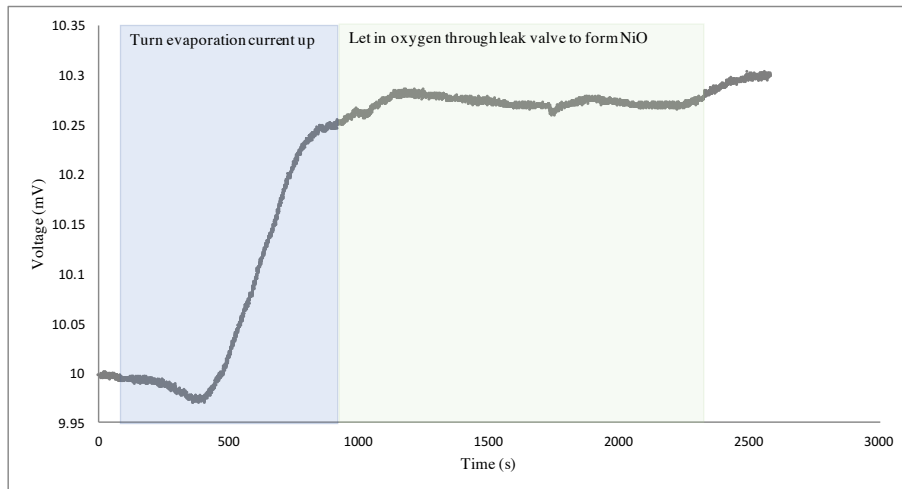
7.2   Results and analysis

Fig.9: Voltage across Cu-surface sample changing during NiO deposition on copper substrate. In the blue region, the evaporation current is turned up to about $30A$ and once the QCM observed $0.2\mathring{A}$ of Ni deposition, oxygen is let into the chamber at about $1.6 \times 10^{-6} Torr$.

Like the deposition described in Section 6, the first sudden change happens before the QCM observes any thickness change. However, at this time, the Ni adsorbate increases the resistance of the copper surface. It is known that although copper and nickel are next to each other in the periodic table, they sometimes show opposite properties [10]. It will take some time to read more literature on how nickel and copper act as substrates and adsorbates. However this is a very interesting phenomena to look at into, one experiment yields too little information to draw any conclusions.

In **Fig.10**, the change in resistance with thickness of NiO is plotted. A sharp increase in sample resistance is seen before $0.5\mathring{A}$, and after it, a sharp decrease is observed. At about $1.5\mathring{A}$, the resistance stabilizes. Again, working with one data set makes it difficult to draw any meaningful conclusions. More experiments are needed to look at into the relationship between sample resistance and NiO adsorption.
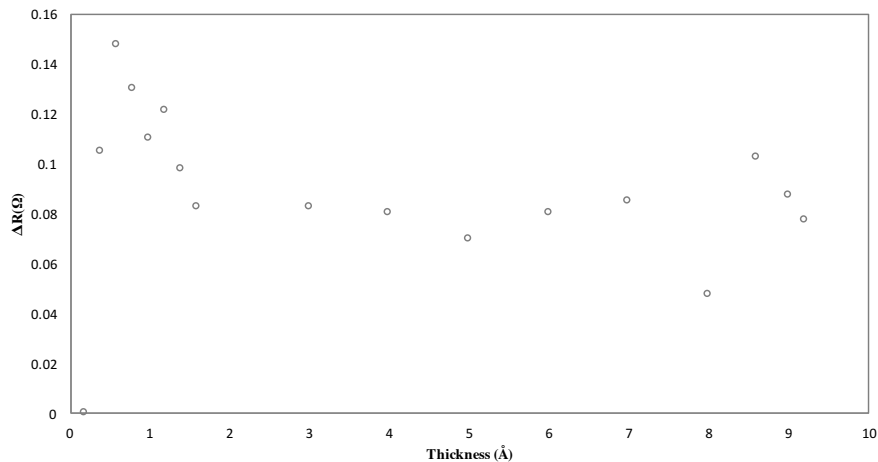

Fig.10: Resistance change of the sample since QCM observed $0.2\mathring{A}$ thickness of Ni.

Our post-NiO deposition Auger ratios for sample 3 showed us that the Cu layer was completely covered, as we had a non-zero $\frac{[O]}{[Cu]}$ ratio of $\sim .14$ before the NiO deposition, but could see no Cu signal at all on the final Auger. After the deposition, the $\frac{[O]}{[Ni]}$ ratio was ~ 2.1, which is consistent with Netzer's findings, which supports the claim that we did successfully deposit NiO on the surface [9]. (<u>Note</u>: Auger ratios averaged from files 02AU19_G.aug through 02AU19_K.aug)

8   Conclusion

The first aim of this research was to see if we could grow NiO in our lab by evaporating Ni onto different metallic substrates in an O_2 atmosphere. We can conclude based on our consistent Auger ratios of $\frac{[O]}{[Ni]}$ that we did in fact deposit NiO onto our sample, under various different conditions and onto different metallic substrates. We used $\frac{[O]}{[Ni]}$ Auger ratios from Netzer's 1975 paper discussing NiO as a benchmark for appropriate levels of O_2 to Ni in a NiO surface [9]. We also wanted to determine what conditions were necessary in order to grow NiO with our current setup; through our experiments on both Ni and Cu we were able to establish workable exposures and settings for doing just so.

The second goal was to measure the change in resistance across the sample during NiO depositions on different types of metallic substrate, namely Ni and Cu. We were able to use LIA scans to observe the

changes in voltage (and correspondingly, resistance) across the top layers of each sample. We measured the impact of temperature differences on our voltage measurements in order to understand the stable conditions we would need to get reliable voltage readings. We went into the UHV chamber and fixed various electrical contact issues in order to establish reliable connections for our resistance readings. Over the course of two months, we were able to identify a pattern in voltage changes during NiO deposition on Ni substrate described in **Fig.7**, and began a series of experiments to repeat this with Cu (which we were not able to finish). There are certainly more experiments to be done to better characterize the dependence of surface resistance of Ni substrate and Cu substrate and the coverage and thickness of NiO adsorbate (see more detail in Sections 6 and 7).

References

[1] Glenny, D., Huang, J., Livermore, S., *Summer 2019 Laboratory Notebook 1.* **11-13** (2019).

[2] Tobin, R.G., *Surf. Sci.* **502-503**, 374 (2002)

[3] Tobin, R.G., *Surf. Sci.* **524**, 183, (2003)

[4] P.H. Holloway and J.B. Hudson, *Surf. Sci.* **123-140**, 43, (1974)

[5] Glenny, D., Huang, J., Livermore, S., *Summer 2019 Laboratory Notebook 1.* **48** (2019)

[6] S.M. Rossnagel and T.S. Kuan, *J. Vac. Sci. Technol., B: Mictroelectron. Nanometer Struct.* **22**, 240(2004)

[7] M. Hein and D. Schumacher, *J. Phys. D: Appl. Phys.* **28**, 1937(1995)

[8] D. Schumacher and D. Stark, *Surf. Sci.* **123**, 384(1982)

[9] F.P. Netzer and M. Prutton, *J. Phys. C: Solid State Phys* **8**, 2401(1975)

[10] Chapter 6 Effects of Adsorption on Some Fundamental Substrate Properties, Editor(s): J. Bénard, Y. Berthier, F. Delarnare, E. Hondros, M. Huber, P. Marcus, A. Masson, J. Oudar, G.E. Rhead, *Studies in Surface Science and Catalysis*, Elsevier, **150-176**, 13 (1983)

[11] Tobin, R.G., *March-August 2002 Lab Notes.* **109-113** (2002).